Korean J. of Chem. Eng., **7**(1) (1990) 31-39

BUBBLE AND GAS HOLDUP CHARACTERISTICS IN A BUBBLE COLUMN OF CMC SOLUTION

Yun Soo MOK*, Young Han KIM and Sang Yeul KIM**

Department of Chemical Engineering, Dong-A University, 840, Hadan-dong, Saha-gu, Pusan, Korea
*Department of Industrial Safety Engineering, Pusan National Institute of Technology,
1268, Daeyeun 6-dong, Nam-gu, Pusan, Korea
(Received 27 February 1989 • accepted 24 July 1989)

Abstract—The local bubble behavior such as holdup, bubble frequency, bubble size and rising velocity in a bubble column of CMC solution was measured using the electroresistivity probe technique, and the effects of gas velocity and CMC concentration on the behavior were investigated. Also, the total gas holdup was measured from the liquid level in the column, and its relation with gas velocity and CMC concentration was studied. Two correlations of mean bubble size and total gas holdup with dimensionless groups, composed of gas velocity and physical properties of gas and liquid, were obtained from the experimental results.

INTRODUCTION

The bubble column is widely used in the chemical processes, since its operating cost is low and heat and mass transfer rates are higher than those of the other equipments owing to the large gas-liquid interfacial area. It also has an advantage giving an easy control of the residence time of liquid phase. Moreover, its maintenance is easy, because it has no moving part and problem caused by corrosion and clogging. Recently it is also used as a bioreactor.

The flow regime, coalescence behavior of bubble, gas holdup, interfacial area and heat and mass transfer coefficients are the important factors in the design of bubble columns, and the bubble diameter, bubble rising velocity, bubble size distribution and bubble velocity distribution are closely related to the column operation.

Many studies have been conducted to obtain the correlation for the prediction of gas holdup in the bubble column, and in the most of the studies the holdup was measured by the pressure difference or liquid level difference at the top and bottom of the column. It is simple and easy to measure the gas holdup, but it does not give any information on the bubble behavior and the local gas holdup in the column.

The observation of bubble behavior in a bubble column can be performed by several different methods. The photographic method takes picture of the bubble and measures the size and distribution. The electroresistivity method utilizes an electric probe installed inside the column and measures the resistance in the gas and liquid phases. Besides, the electrooptical probe method and light scattering method have also been adopted in the studies of bubble behavior.

An early report using the electroresistivity method was published by Neal and Bankoff [1]. In the study, the local gas holdup and bubble behavior were observed with a single tip probe in a nitrogen-mercury system. Two groups of investigators [2,3] compared the dual tip electroresistivity method with the photographic method, and found that both methods show relatively good agreement in the measurement of bubble size. Also a study on the bubble behavior and gas holdup in a slurry bubble column using dual tip electroresistivity method was presented by Yasunishi et al. [4].

The gas holdup and bubble behavior in the non-Newtonian liquid have been studied by many researchers, since their values can not be predicted from the correlations between the gas holdup and the column operating condition and physical properties of liquid for the Newtonian liquid systems.

The gas holdup in a carboxymethyl cellulose (CMC) solution was measured by Nakanoh and Yoshida [5]. Their experimental data were correlated with the dimensionless groups of Bond, Galilei and Froude which were also used for the Newtonian liquid. The variation of gas holdup with gas velocities in CMC

To whom all correspondences should be addressed.

solution was observed by Franz et al. [6]. The increase of holdup with increasing gas velocity was explained with the fact that the column acts like an aerator, and the aerator effect reduces with increasing CMC concentration. The effect of hole size of perforated plate on the gas holdup has also been studied, and it was found that the large holes result in the low gas holdup. The effect of CMC concentration on gas holdup diminishes for the large hole perforated plate. The effects of gas velocity, CMC concentration and hole size on the Sauter mean bubble diameter were also investigated in the study. Another correlation on the gas holdup with gas velocity and effective viscosity of the CMC solution was obtained by Godbole et al. [7]. The gas velocity has the same influence on the gas holdup as shown in the previous studies [5,6], and the high effective viscosity is leading to low gas holdup.

The effect of the column height on the gas holdup for the CMC solution was studied by Haque et al. [8]. The possibility of bubble coalescence is high as the column height increases owing to the high frequency of collision between bubbles, and it results in large bubbles. In the study, an explanation on the decreasing bubble diameter with increasing gas velocity was given as a contrary result to the Newtonian liquid systems. The explanation is that high gas velocity gives high shear rate, leading to low effective viscosity in CMC solutions, and the bubbles are susceptible to break.

In this study, the bubble behavior such as bubble size and bubble rising velocity in a bubble column of CMC solution was measured with an electroresistivity dual-tip probe. The obtained signals were digitized and processed with a microcomputer, and the local gas holdup, bubble frequency, bubble rising velocity, bubble size, cross-sectionally averaged gas holdup and bubble size distribution were calculated from the processed data. And the total gas holdup was determined by the liquid level method.

The effects of gas velocity and CMC concentration on the bubble properties and total gas holdup were investigated, and the correlations of mean bubble size and total gas holdup were formulated from the experimental values.

EXPERIMENTAL

1. Experimental setup

The bubble column is composed of a column, a perforated plate and a bottom section. The column is 14 cm in diameter and 200 cm high, and the bottom section has the same diameter and 20 cm in depth. All of them are made of polymethyl metacrylate, and connected with flange joint. The perforated plate has 51 holes of 0.3 mm diameter in the equilateral triangular pitch through the whole area inside the column. A brief arrangement of the experimental setup is shown in Figure 1.

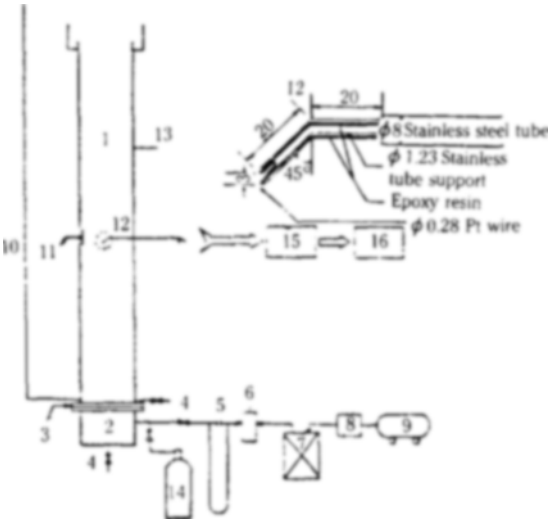

1. Column
2. Air chamber
3. Perforated plate
4. Valve
5. Manometer
6. Regulator
7. Saturator
8. Oil water separator
9. Compressor
10. Manometer
11. Counter electrode
12. Electro-resistivity probe
13. Sampling
14. N_2 cylinder
15. Data instrumentation unit
16. Data processing unit

Fig. 1. Schematic diagram of experimental apparatus.

A barometric manometer tap is installed at the bottom of the column. A movable probe in the radial direction is placed at the position of 60 cm from the perforated plate. The detail of the probe is illustrated in the subdiagram of Figure 1. The probe is made of platinum wire of 0.28 mm in diameter, sharpened and coated with epoxy resin for insulation except the probe tip. The wire is supported with a stainless steel tube of 1.23 mm O.D., and the support tube is bent in 45 degrees downward to minimize the interference of probe in the path of bubbles at the measuring moment. The vertical distance between two tips is 3 mm, and the bubble rising velocity is calculated from the distance and the difference of the initial contact time of bubble and the tips. A counter electrode is made of a stainless steel plate of 25 mm × 100 mm, and installed on the wall of the column in the opposite side of probe.

The signal in the form of voltage difference be-

Table 1. Physical properties of CMC solutions (25°C)

conc. wt% of CMC in water	density g/cm³	σ dyne/cm	k dyne s^n/cm²	n
0	0.9971	72	0.01	1.0
0.05	0.9971	71.41	0.0133	0.998
0.075	0.9975	71.35	0.0161	0.986
0.10	0.9976	71.25	0.0215	0.939
0.15	0.9978	71.09	0.0281	0.893
0.20	0.9979	70.90	0.0445	0.873
0.30	0.9982	70.53	0.075	0.809

tween the probe tip and counter electrode is fed to an A/D converter after the rectification of high frequency signal.

Air is supplied from a compressor and passed through an oil separator and a water saturator. A set of orifice and manometer is provided for the measurement of air flow rate.

2. Measurement of physical properties

The surface tension of the CMC (1st grade, Junsei Chemical Co., Japan) solution was measured with a du Nouy type surface tensiometer (Fischer, model 20), and the specific gravity was with Baume hydrometer.

The viscosity of CMC solution was expressed with the power law model, as in Eq. (1), and its flow consistency index, k, and flow behavior index, n, were calculated from the measured shear force at the different shear rate using the linear least square technique. The shear force was obtained with concentric cylinder viscometer (Brookfield, model LV). The physical properties of the water and CMC solutions are given in Table 1.

$$\Gamma = k\gamma^n \tag{1}$$

3. Measurement of bubble size and rising velocity

When a bubble passes through the tip of probe, it is detected by the conductivity variation. The bubbles passing the tip are so many and the bubble rising is very fast, and so the conductivity measurement and data collection have to be fast. A brief diagram of signal processing is given in Figure 2.

A signal function generator supplies the sine wave signal of 90 kHz and 10 volts peak-to-peak to the counter electrode. The continuous signal measured through the probe is varied while a gas bubble contacts the probe tip. The detected signal is rectified and amplified to feed an A/D converter (MetraByte, model DAS-8) installed in an IBM PC/XT microcomputer.

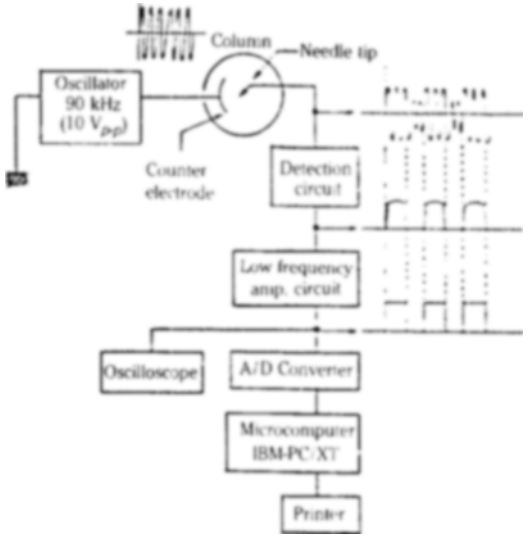

Fig. 2. Diagram of signal processing for electroresistivity probe.

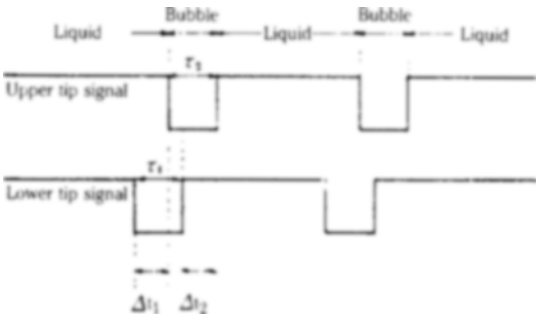

Fig. 3. Signal sequences of bubble detected by the electroresistivity probe.

The digitized signal was sampled in every 376.3 microseconds and stored in the main memory of the computer. An one time experiment was conducted for 25.4 seconds because of the main memory limitation, and the obtained data were transferred into the auxiliary memory device after a set of data was gathered. The memorized data were retrieved and analyzed to calculate the number of bubbles for the sampling period, the bubble length and the bubble rising velocity.

The signals from the upper and lower tips of the probe should be matched for a single bubble as shown in Figure 3. Yasunishi et al. [4] used the several criteria to find a pair of bubble signals for a single bubble, and the modified criteria were applied in this study.

1. $\Delta t_1 < 1.5\Delta t_2$
2. $\Delta t_2 < 1.5\Delta t_1$
3. $0.75 \leqq 2\tau_1/(\tau_1+\tau_2) \leqq 1.25$

The first and second conditions were made considering that the gap of two tips is only 3 mm and a matched bubble signal should not have a large difference in the time delays of the on and off contact. The third condition was made from the fact that the possibility of bubble coalescence or bubble breakup within the tip clearance is very small.

The experiment was conducted for the superficial gas velocities between 0.96 and 5.04 cm/sec and the CMC concentration of liquid was varied from 0.05 to 0.3 wt%.

RESULTS AND DISCUSSION

1. Bubble behavior

1.1. Local gas holdup and bubble frequency

The local gas holdup at the height of 60 cm from the perforated plate was measured at the different radial positions. The radial positions were selected in the equal distance of 1.4 cm except the very wall position where the tip of the bent probe could not be located. In the case the probe was placed at 0.5 cm inside from the wall.

The radial distribution of local gas holdup for the various concentrations of CMC solution is shown in Figure 4. At high gas flow rate, the local gas holdup was also high for all the CMC concentrations. The bubble frequency distribution for the same solutions is shown in Figure 5, and the variation trends are similar to the local gas holdup. The distribution of local gas holdup and bubble frequency in the radial direction was nearly uniform except for the points near the wall at the low CMC concentration and low gas velocity such as 0.2% or less and 4.03 cm/sec or lower, respectively. At the high velocity and concentration, the distribution has a half parabola shape with a maximum value in the center of the column. At high gas velocity, the wall effect is stronger than that of low velocity, and the parabola shape is more apparent. The same result has been reported in the air-water

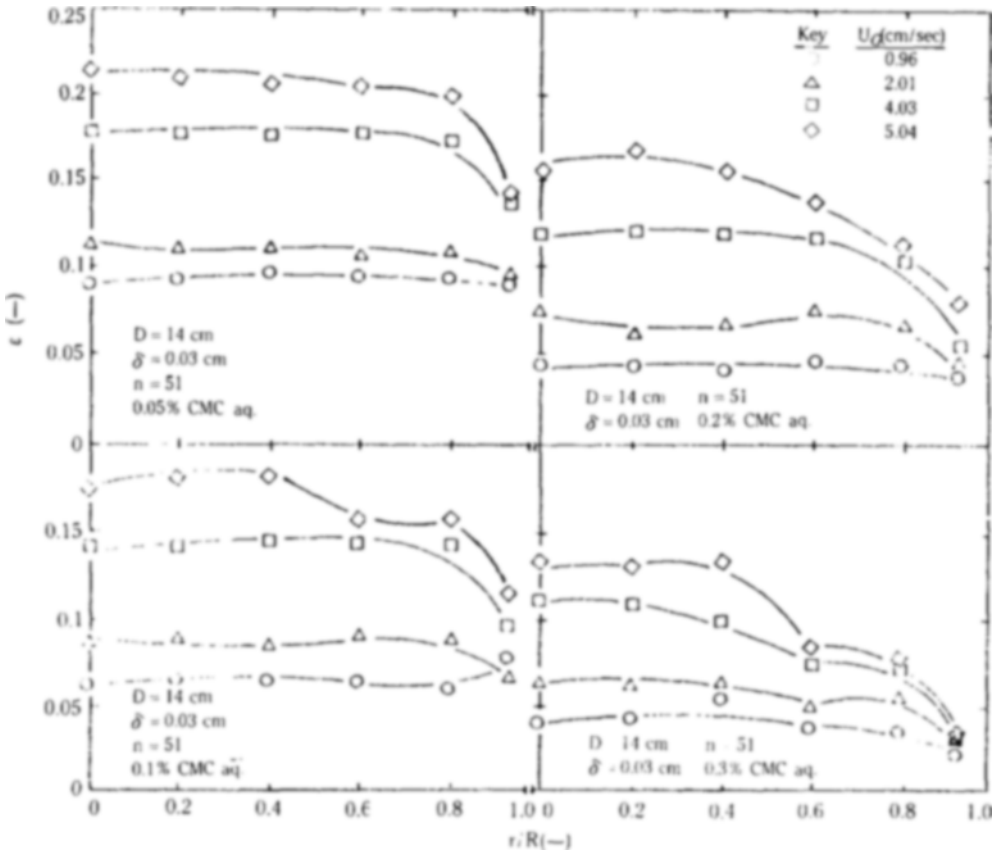

Fig. 4. Radial distribution of local gas holdup.

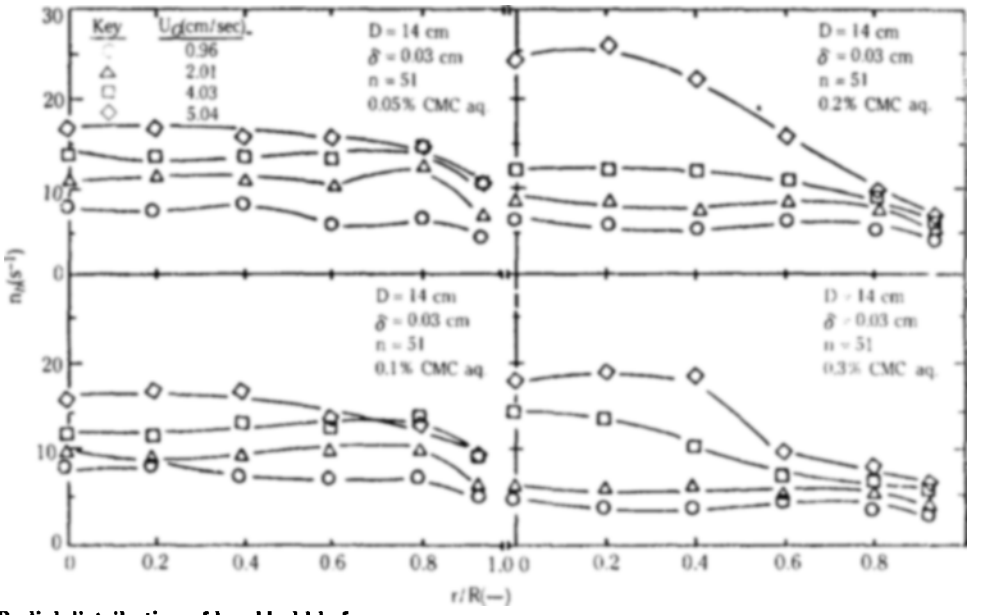

Fig. 5. Radial distribution of local bubble frequency.

system [4].

The unique behavior of CMC solution is appeared in high concentration of CMC solution. The effective viscosity of the CMC solution decreases as the shear rate increases, and higher shear rates are obtained at higher gas velocities. The relation can be found from the definition of the effective viscosity in the power law model of Ostwald-de Waele [8] for the pseudoplastic liquid as given in Eq. (2).

$$\mu_{eff}=k\,\gamma^{n-1} \tag{2}$$

Since the flow behavior index, n, is far smaller than unity for the high concentration of CMC solution, the effective viscosity is smaller than low concentration solution. It accounts for the parabola shape distribution of local gas holdup for the high concentration CMC solution. The apparent parabola distribution in water having low viscosity also indicates the relation between the local holdup distribution and viscosity.

1-2. Cross-sectionally averaged gas holdup

The cross-sectionally averaged gas holdup can be defined as

$$\bar{\varepsilon}=\frac{2}{R^2}\int_0^R \varepsilon r dr \tag{3}$$

However, the local gas holdup can not be measured continuously along the radial position. From the measurement at the discrete radial position, the averaged gas holdup can be redefined as Eq. (4).

$$\bar{\varepsilon}=\frac{2}{R^2}\sum_i \varepsilon_i r_i \Delta r \tag{4}$$

The cross-sectionally averaged gas holdup in the various concentrations of CMC solution and different gas velocities is plotted in Figure 6, and it shows that the holdup increases with increasing gas velocity, which is the same tendency as in the total gas holdup. At the high CMC concentration, the cross-sectionally averaged gas holdup is found to be small. It is because the effective viscosity of the CMC solution lowers while the concentration increases. The holdup in 0.3% CMC solution is even smaller than that of water. At low CMC concentration, 0.2% or less, the viscosity is higher than that of water, therefore the holdup of water is lower than that of the solutions. The same result is shown in the total gas holdup.

1-3. Distribution of bubble size

The mean bubble size at the center of the column in various concentrations of CMC solution with different gas velocities are shown in Figure 7. The bigger the bubble size is, the higher the gas velocity, and it can be found also in Ueki [9]'s work. The effect of viscosity on the mean bubble size is not significant except for 0.3% CMC solution. In 0.3% CMC solution the mean size of bubble is larger than that of other solutions, and it is resulted from the low effective viscosity of the solution.

A correlation of the mean bubble diameter, arithmetically averaged value of the vertical bubble length,

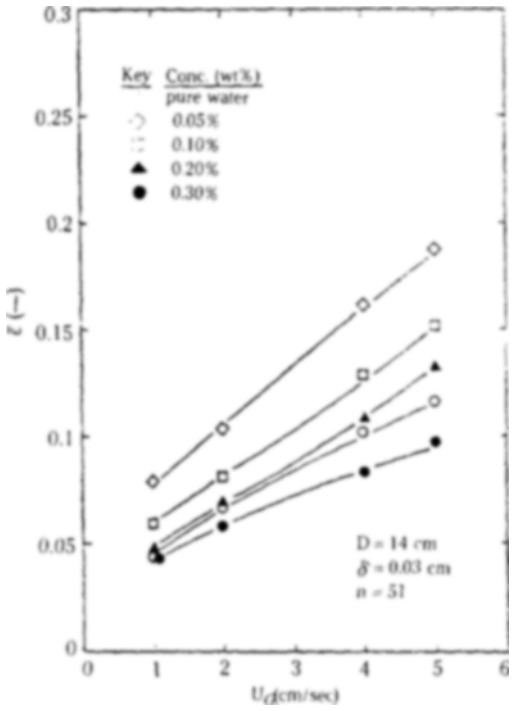

Fig. 6. Effect of gas velocity on cross-sectionally averaged gas holdup.

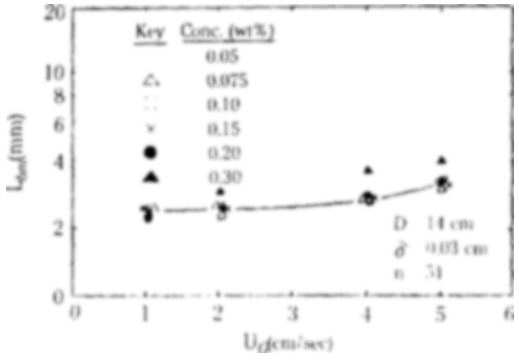

Fig. 7. Effect of gas velocity on mean bubble diameter for different CMC aqueous solutions at the center of column.

in terms of dimensionless groups has been reported by Miyahara et al. [10], and the same form of equation was used in this study. The coefficient and exponent of Eq. (5) was obtained from the measured mean bubble diameter using the least square method.

$$L_{bm}(\rho_L g/\delta\sigma)^{1/3} = 2.61\,(We/Fr^{0.5})^{-0.182} \qquad (5)$$

A plot for the correlation is shown in Figure 8, and the values in 0.3% CMC solution were not included in it

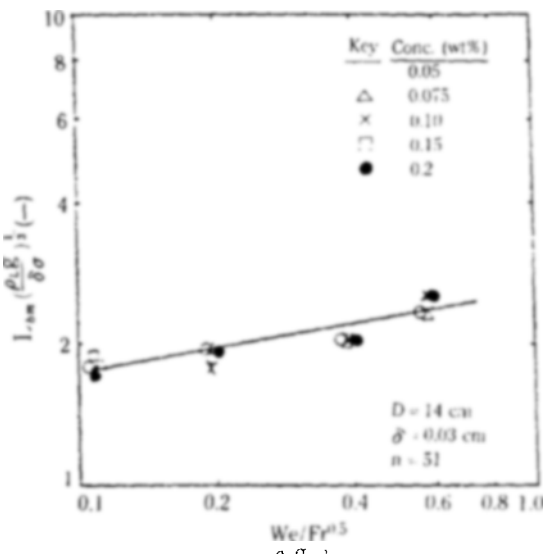

Fig. 8. Correlation of $L_{bm}(\frac{\rho_L g}{\delta\sigma})^{\frac{1}{3}}$ and We/Fr$^{0.5}$.

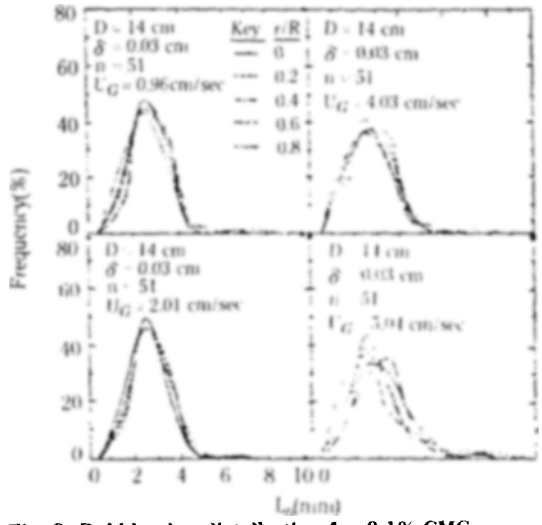

Fig. 9. Bubble size distribution for 0.1% CMC aqueous solution at different radial locations and gas velocities.

since they are quite different from those of lower concentration solutions. The standard deviation and the correlation coefficient of the fitting are 0.12 and 0.89, respectively.

The bubble size distribution of 0.1% CMC solution in the radial direction is shown in Figure 9. At low gas velocities the distribution is nearly same regardless of the radial location, but the size distribution moves to wider bubble distribution at high velocities. The coalescence of small bubbles, occurring from the begin-

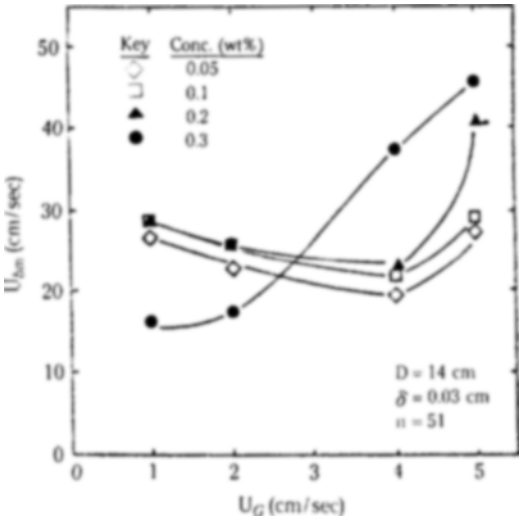

Fig. 10. Effect of gas velocity on mean bubble rising velocity for different CMC aqueous solutions ($\frac{r}{R}$ = 0.2).

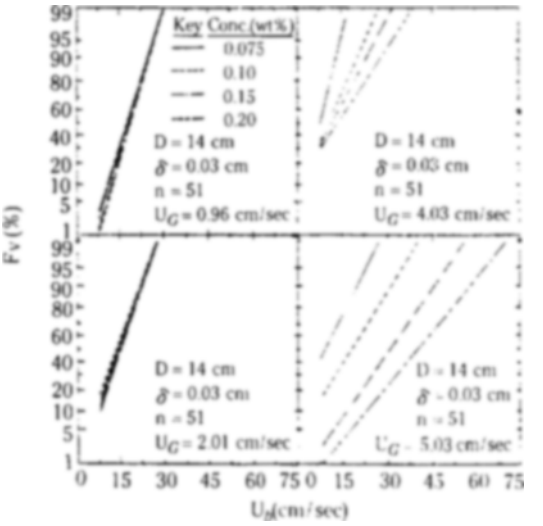

Fig. 11. Cumulative bubble rising velocity distribution for different CMC aqueous solutions and gas velocities at the center of column.

ning of the bubble formation, is responsible for the large bubble at high velocity.

1-4. Bubble rising velocity

The mean bubble rising velocity for the different gas velocities and CMC concentrations is shown in Figure 10, and generally it decreases while the gas velocity increases excepting the cases of high gas velocity and high CMC concentration. The same results have been obtained by Nicklin [11], and he explained that it is because the bubbles are becoming densely packed. At high gas velocity and high CMC concentration, the effective viscosity of the solution is low in which the drag force is small, and bubbles rise fast. For 0.3% CMC solution the bubble rising velocity increases with gas velocity contrarily to other solutions, and it is because the effect of the reduction of the effective viscosity is stronger than that of dense bubble population.

For the better observation of the bubble rising velocity distribution, the cumulative bubble rising velocity distribution is prepared as seen in Figure 11. At low gas velocity the distribution of bubble rising velocity has nearly same no matter what the CMC concentration is. For high velocity, however, the distribution is broadened, and at high CMC concentration it is even broader. It also relates with the low effective viscosity.

2. Total gas holdup

The total gas holdup was measured with a liquid level manometer. A plot of gas holdup versus CMC concentration at the different gas velocites is shown in Figure 12. The total gas holdup in CMC solution increases as gas velocity increases. The effect of CMC concentration on the total gas holdup is not observed at low gas velocities. At high gas velocities, however,

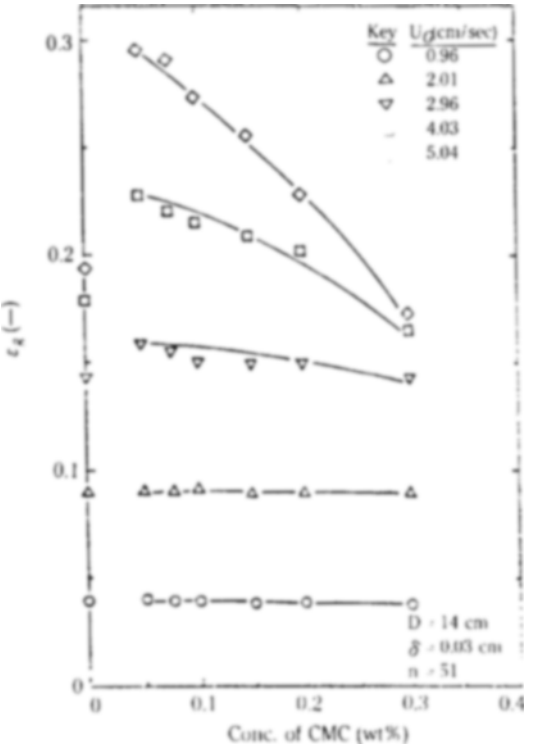

Fig. 12. Effect of CMC concentrations and gas velocities on total gas holdup.

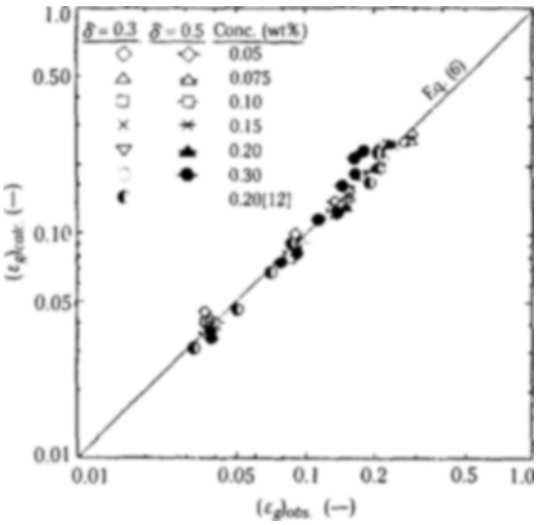

Fig. 13. Comparison of the experimental and calculated gas holdup.

the effect of CMC concentration on gas holdup is significant and the holdup decreases as the concentration increases. The pseudoplastic behavior of CMC solution is responsible for the result, and it has been discussed in the explanation for the cross-sectionally averaged gas holdup.

The gas velocity, physical properties of solution and hole size of the perforated plate affect the gas holdup of bubble column and the gas holdup can be correlated with the factors. An experimental correlation between the gas holdup and the affecting factors in the form of dimensionless groups was obtained as follows;

$$\varepsilon_g = 0.107 \times 10^{-4} \mathrm{Re}_G^{1.09} \mathrm{Ga}^{0.096} (\delta/\mathrm{D})^{-0.19} \quad (6)$$

The coefficient and exponents in the equation were calculated by the least square method using matrix pseudo-inversion. The standard deviation and the coefficient of determination of the fitting are 0.015 and 0.98, respectively.

The comparison of the calculated holdup from Eq.(6) with the experimental results of this study and published data [12] is given in Figure 13, and it shows a good agreement.

CONCLUSION

The local bubble behavior and total gas holdup in a bubble column of CMC solution were obtained by the electroresistivity probe technique and liquid level measuring.

The high gas velocity up to 5.04 cm/sec raises the local gas holdup and bubble frequency. The distribution of local gas holdup in the radial direction is nearly uniform at low gas velocity and low CMC concentration. The cross-sectionally averaged gas holdup increases with increasing gas velocity, while it decreases with increasing CMC concentration up to 0.3 wt%. The mean bubble size is nearly same at low gas velocity and low concentration. At high gas velocity and CMC concentration, the effective viscosity is low and the bubble coalescence is promoted, and it leads to the large bubbles. The mean bubble rising velocity lowers when the gas velocity becomes higher for the low gas velocity and low CMC concentration. At high gas velocity and high CMC concentration the same increase of the bubble rising velocity as found in the mean bubble size is obtained.

The total gas holdup increases as the gas velocity increases, but it diminishes in the high CMC concentration solution even as the velocity increases.

Two correlations with low deviation for the mean bubble diameter and the total gas holdup were made from the experimental results.

NOMENCLATURE

D : column diameter, [cm]
Fr : Froude number $[=U_G/(gD)^{0.5}]$
Fv : cumulative bubble velocity distribution, [%]
Ga : Galilei number $(=gD^3/\nu_{eff}^2)$
g : gravitational acceleration, [cm/s^2]
k : fluid consistency index, [dyne s^n/cm^2]
L_b : vertical bubble length, [cm]
L_{bm} : arithmatic mean of bubble diameter, [cm]
n : flow behavior index, or number of holes in perforated plate
n_b : local bubble frequency, [s^{-1}]
R : column radius, [cm]
Re_G : Reynolds number of gas $(=DU_G\rho_G/\mu_G)$
r : radial distance from center, [cm]
t : time, [s]
U_b : local bubble rising velocity, [cm/s]
U_{bm} : arithmatic mean of bubble rising velocity, [cm/s]
U_G : superficial gas velocity, [cm/s]
We : Weber number $(=\delta U_G^2\rho_L/\sigma)$

Greek Letters

Γ : shear stress, [dyne/cm^2]
γ : shear rate, [s^{-1}]
δ : hole size of perforated plate, [cm]
ε : local gas holdup
$\bar{\varepsilon}$: cross-sectionally averaged gas holdup
ε_g : total gas holdup

μ_G : gas viscosity, [g/cm·s]
μ_{eff} : effective liquid viscosity, [g/cm·s]
ν_{eff} : effective kinematic viscosity, [cm^2/s]
ρ_L : liquid density, [g/cm^3]
ρ_G : gas density, [g/cm^3]
σ : surface tension, [dyne/cm]
τ : bubble duration time at a probe tip, [s]

REFERENCES

1. Neal, L.G. and Bankoff, S.G.: *AIChE J.*, **9,** 490 (1963).
2. Yamashita, F., Mori, Y. and Fujita, S.: *J. Chem. Eng. Japan,* **12,** 5 (1979).
3. Buchholz, R. and Schugerl, K.: *European J. Appl. Microbiol. Biotechnol.*, **6,** 301 (1979).
4. Yasunishi, A., Fukuma, M. and Muroyama, K.: *J. Chem. Eng. Japan,* **19,** 444 (1986).
5. Nakanoh, M. and Yoshida, F.: *Ind. Eng. Chem. Process Des. Dev.*, **19,** 190 (1980).
6. Franz, K., Buchholz, R. and Schugerl, K.: *Chem. Eng. Commun.*, **5,** 187 (1980).
7. Godbole, S.P., Schumpe, A. and Shah, Y.T.: *AIChE J.*, **30,** 213 (1984).
8. Haque, M.W., Nigam, K.D.P., Viswanathan, K. and Joshi, J.B.: *Ind. Eng. Chem. Res.*, **26,** 86 (1987).
9. Ueki, S.: Ph. D. Dissertation, Univ. of Tokyo, Tokyo, Japan (1969).
10. Miyahara, T., Matsuba, Y. and Takahashi, T.: *Kagaku Kogaku Ronbunshu,* **8,** 13 (1982).
11. Nicklin, D.J.: *Chem. Eng. Sci.*, **17,** 693 (1962).
12. Shah, Y.T., Kelkar, B.G., Godbole, S.P. and Deckwer, W.-D.: *AIChE J.*, **28,** 353 (1982).